

DENSIFICATION BEHAVIOR OF SnO₂-GLASS COMPOSITES DEVELOPED FROM THE INCORPORATION OF SILICA XEROGEL AND SnO₂

H. Aripin^{1*}, Seitaro Mitsudo², I Nyoman Sudiana³, Edvin Priatna⁴, Hikamatsu Kikuchi⁵, Svilen Sabchevski⁶

¹*Faculty of Learning Teacher and Education Science, Siliwangi University, Tasikmalaya, Indonesia*

²*Research Center for Development of Far Infrared Region (FIR Center), University of Fukui, Fukui, Japan*

³*Department of Physics, Faculty of Mathematics and Natural Sciences, University of Haluoleo, Kendari, Indonesia*

⁴*Department of Electrical Engineering, Faculty of Engineering, Siliwangi University, Tasikmalaya, Indonesia*

⁵*Department of Applied Physics, Faculty of Engineering, University of Fukui, Fukui, Japan*

⁶*Laboratory of Plasma Physics and Engineering, Institute of Electronics of the Bulgarian Academy of Sciences, Bulgaria*

(Received: December 2015 / Revised: January 2016 / Accepted: February 2016)

ABSTRACT

In this investigation, SnO₂-glass composites were produced by mixing SnO₂ and amorphous silica xerogel (SX) extracted from sago waste ash. The composition was prepared by adding 5 mol% of SnO₂ into SX; the samples were dry pressed and sintered in a temperature range between room temperature and 1500°C. Their properties were characterized on the basis of the experimental data obtained using Archimedes' principle, X-ray diffraction (XRD), Fourier transformed infra-red (FTIR), and a scanning electron microscopy (SEM). It was found that the bulk density increased along with the sintering temperature. In the temperature range from 1300°C to 1500°C, the glass ceramic reached a bulk density of about 2.5 g/cm³. The results of the interpretation of XRD patterns, FTIR spectra, and SEM images allow us to conclude that this increase in density was due to an increased degree of crystallinity of SnO₂ in the silica xerogel composite.

Keywords: Amorphous silica xerogel; Density; Glass composite; Sintering temperature; SnO₂

1. INTRODUCTION

Silica xerogel (SX) is one of the colloidal silica materials that have a rigid three-dimensional network. It changes from a fully amorphous state to a partially crystallized state of cristobalite at 800°C, and a fully crystallized state at 1100°C (Aripin et al., 2011; Aripin et al., 2013). Total The crystallization process significantly reduces the large amount of texture pores that exist in SX, and eventually decreases their specific surface area (SSA) from 350 cm²/g to 8 cm²/g. In addition, the degree of crystallinity of cristobalite greatly affects the grain growth of SX. The result is an increase of density from 0.4 g/cm³ at room temperature to 2.2 g/cm³ at temperatures above 1000°C (Aripin et al., 2012). SX is also used as an appropriate material when a high

*Corresponding author's email: aripin@unsil.ac.id, Tel. +62-265-330634, Fax. +62-265-325812
Permalink/DOI: <http://dx.doi.org/10.14716/ijtech.v7i3.2903>

optical transparency and a very low loss (about 0.2 dB/km at a wavelength of 1.55 μm) are required (Kim et al., 2006). However, the large quantity of cristoballite in SX at high temperatures gives rise not only to embrittlement and loss in strength of the ceramics, but also leads to a complete loss of thermal-shock resistance. In order to overcome this failing, additives to suppress the formation of cracks were used.

Thermal expansion behavior is one of the most important aspects of a proper optical design and construction. A controlled expansion can help prevent the formation of cracks and pores. In this study, SnO₂ was employed as an additive for improving the expansion behavior of silica-based glass ceramic systems. The aim was to find, through experiments, the appropriate technological parameters for producing nanosized SiO₂/SnO₂ and to evaluate the effect of differing amounts of SnO₂ on the properties of silica glass ceramic. Additionally, the study focused on the relationships between the microstructural changes and the sintering temperature of nano-SiO₂/SnO₂ ceramic. Due to the photorefractive properties of SnO₂, its incorporation in SiO₂ makes these structures appropriate for application in silica-based integrated optics.

2. EXPERIMENTAL

2.1. The Silica Xerogel and SnO₂ Composite Preparation

Amorphous SX was extracted from sago waste (a solid residue left behind after the starch has been washed out), which was obtained from the sago processing plant in Kendari, Indonesia. The detailed extraction procedures were elaborated in previous studies (Aripin et al., 2011; Affandi et al., 2009). The composite powder was prepared using SX and SnO₂ derived from SnCl₂·2H₂O. 1 g of SnCl₂·2H₂O was dissolved in a water-ethanol solution containing 50 mL ethanol and 50 mL deionized water, which was then stirred at a temperature of 80°C for one hour. 19 g of SX powder was then added slowly into the solution containing Sn²⁺ ions, which had been continuously stirred at 50°C for six hours. The pH of the mixed solution was adjusted to 2.8 to obtain a white precipitate of tin hydroxide. The mixture solution was heated at 80°C until all solvent was evaporated; the resultant powder of SiO₂/SnO₂ was dried in an oven at a temperature of 120°C for two hours. We will refer to the sample prepared as SX-5 mol%SnO₂. To mold cylindrical samples with a diameter of 10 mm and a thickness of 7 mm, we used experimental procedures from a previous study (Aripin et al., 2012).

2.2. Sintering the Green Body of Silica Xerogel and SnO₂ Composite

Experiments in green body sintering were carried out using an electric furnace system at temperatures ranging from 800 to 1500°C. A controlled heating rate of 5°C/min was maintained up to the desired temperature, which was then kept constant for two hours. Cooling was performed by natural convection after turning the furnace off and leaving the samples inside.

2.3. Methodology for Characterizing the Structure of Silica Xerogel/SnO₂ Ceramic

After sintering, important characteristics such as density and porosity were measured. The experimental procedures to measure these were similar to those of a previous study (Aripin et al., 2011). The crystal structure of all samples was characterized at room temperature, using a Smartlab X-ray diffractometer operated at a voltage of 40 kV and a current of 30 mA. The intensity of the diffracted radiation was registered as a function of the diffraction angle, ranging from 10 to 90 degrees using Cu K α radiation with a wavelength of 0.15418 nm. The surface morphology of the sample was then examined by a scanning electron microscope (SEM) JOEL JSM-6400. Images were taken at a magnification of 5000 x at 15 kV. The Fourier transformed infra-red (FTIR) spectra were recorded using IRPrestige-21 in the 400–4000 cm⁻¹ wave number range by the KBr method.

3. RESULTS AND DISCUSSION

Figure 1 shows some representative XRD patterns of dried powder sample without sintering (untreated), and of samples sintered at a temperature range of 800°C to 1500°C. Well-separated characteristic peaks of both SX and tin dioxide (SnO_2) can be seen. This observation provides evidence that a direct chemical interaction between SX and SnO_2 does not take place in a composite xerogel.

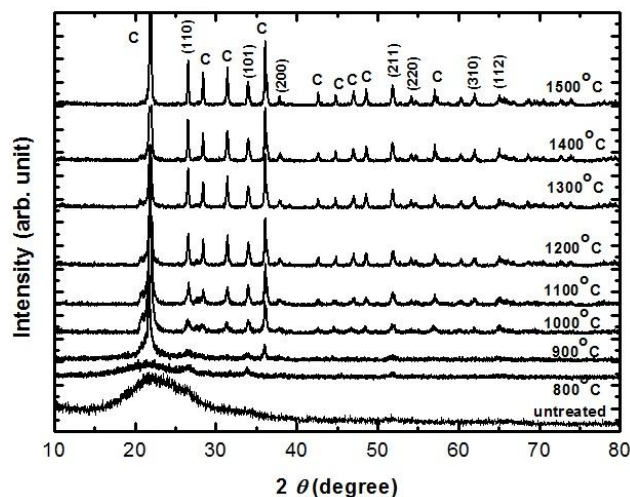


Figure 1 XRD patterns of silica xerogel loaded by 5 mol% SnO_2 and sintered at different temperatures

For the untreated sample, there is one small broad peak at about $2\theta = 22.9^\circ$, which is characteristic for the presence of an amorphous SX. One can see that for the sample sintered at 800°C, there is a pattern similar to the initial (i.e. untreated) sample at the same peak position, but the peak intensity is reduced. At the same temperature, three other weak peaks appear at $2\theta = 26.9^\circ$, 34.1° , and 52.0° , which are assigned to the (110), (101), and (211) planes of the tetragonal rutile SnO_2 crystal (Gaber et al., 2014). At 900°C, two new intense peaks arise at $2\theta = 22^\circ$ and 36° . They are attributed to the (101) planes of the cristobalite structure of silica. This observation indicates that the crystallization of silica occurs at around 900°C, while that of a pure silica system begins at 1400°C (Diaz-Flores et al., 2007). The intensity of cristobalite peaks increases with rises in the sintering temperature. In the range of 1000°C to 1500°C, the peaks at $2\theta = 38.2^\circ$, 54.0° , 62.0° , and 65.0° correspond to (200), (220), (310), and (112) planes of the SnO_2 crystal. These clear peaks are in good agreement with those found in the JCPDS card (411445) (McCarthy & Welton, 1989).

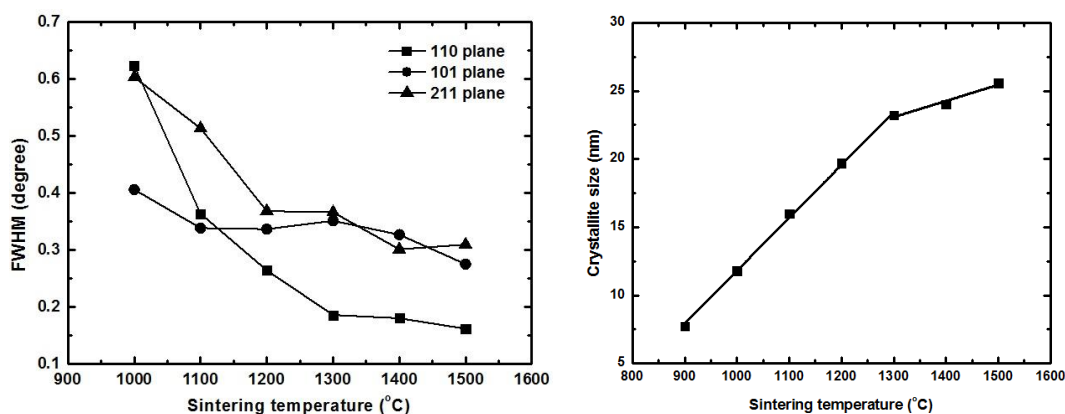


Figure 2 (a) FWHM and (b) crystallite growth of silica xerogel loaded by 5 mol% SnO_2 and sintered at different temperatures

Figure 2a shows the full width at a half maximum (FWHM) of the peaks with highest intensity that correspond to the planes (110), (001), and (211) of SX loaded by 5 mol% SnO₂ and sintered at different temperatures. It can be seen that the width of the peaks decreases with increases in the sintering temperature. This trend is attributed to a growth of the crystallite size of the SnO₂ crystal. As shown in Figure 2b, this size was calculated from the diffraction peaks using Scherrer's formula (Kose et al., 2014):

$$\langle d \rangle = \frac{K\lambda}{\beta \cos \theta} \quad (1)$$

where $\langle d \rangle$ is the mean crystallite size, K is the shape factor, β is the full width at half maximum (FWHM), λ is the wavelength of the X-ray, and θ is the Bragg angle. The crystallite size increases along with the sintering temperature. The slope of the curve, however, is different in the temperature ranges from 900°C to 1300°C and from 1300°C to 1500°C. This indicates a different rate of crystal growth in these temperature intervals. According to Gaber et al. (2014), the rapid growth of crystallite size at temperatures from 900°C to 1300°C is caused by the presence of more agglomerated crystals, whereas the slow growth from 1300°C to 1500°C can be explained by the presence of an almost fully crystallized state of the crystalline SnO₂.

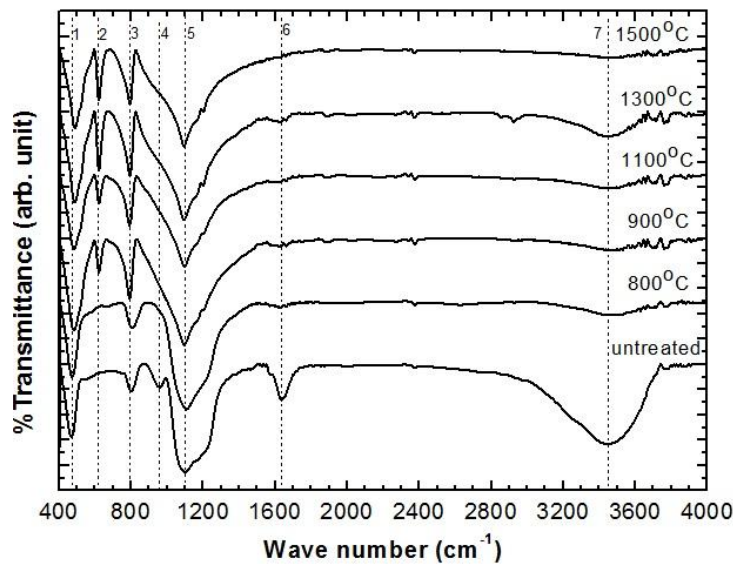


Figure 3 FTIR spectra of silica xerogel loaded by 5 mol% SnO₂ and sintered at different temperatures

Figure 3 shows the Fourier Transform Infra-Red (FTIR) spectra of SX loaded by 5 mol% SnO₂ and sintered at different temperatures. For all samples, the absorption band (peak 1) observed at about 464 cm⁻¹ was attributed to an Si-O-Si bending vibration (Wagh & Ingale, 2002). Peak 2, which appears at 634 cm⁻¹, relates to the O-Sn-O bridge functional groups of SnO₂ (Tan et al., 2011) which occur in samples sintered at temperatures greater than or equal to 900°C. This confirms the presence of SnO₂ as a crystalline phase, and is in agreement with the results of the XRD analysis. For all samples, bands at 802 cm⁻¹ (peak 3) and 1099 cm⁻¹ (peak 5) are assigned, respectively, to the symmetric stretching of the Si-O-Si group and to the asymmetric stretching of the Si-O-Si structural bond of siloxane (Jung et al., 2005). In an untreated sample, peak 4 at around 980 cm⁻¹ corresponds to the presence of an Si-OH group (Wagh & Ingale, 2002). Peak 6, observed at 1620 cm⁻¹, is associated with bending H-O-H bond groups of adsorbed water molecules, while a broad band (peak 7) at 3452 cm⁻¹ is attributed to O-H stretching from

hydroxyl groups that are present on the surface of the material (Yang & Gao, 2006). As the sintering temperature increases, these bands gradually become weaker and disappear at temperatures greater than 800°C.

Figure 4 presents SEM images of SX samples loaded by 5 mol% SnO₂ and sintered at various temperatures. They show how the surface morphology changed when the sintering temperature was raised. The sample sintered at 800°C is characterized by non-uniformity and significant roughness. A salient feature of the samples sintered at 800°C and 900°C is the porosity of the amorphous silica structure. At 1000°C, the surface of the sample is more smooth and uniform, corresponding to the presence of the crystalline cristobalite structure of SX. From 1000°C to 1500°C, the microstructure is characterized by a high degree of agglomeration among fine particles. Crystalline SnO₂ particles are not seen in the microstructure.

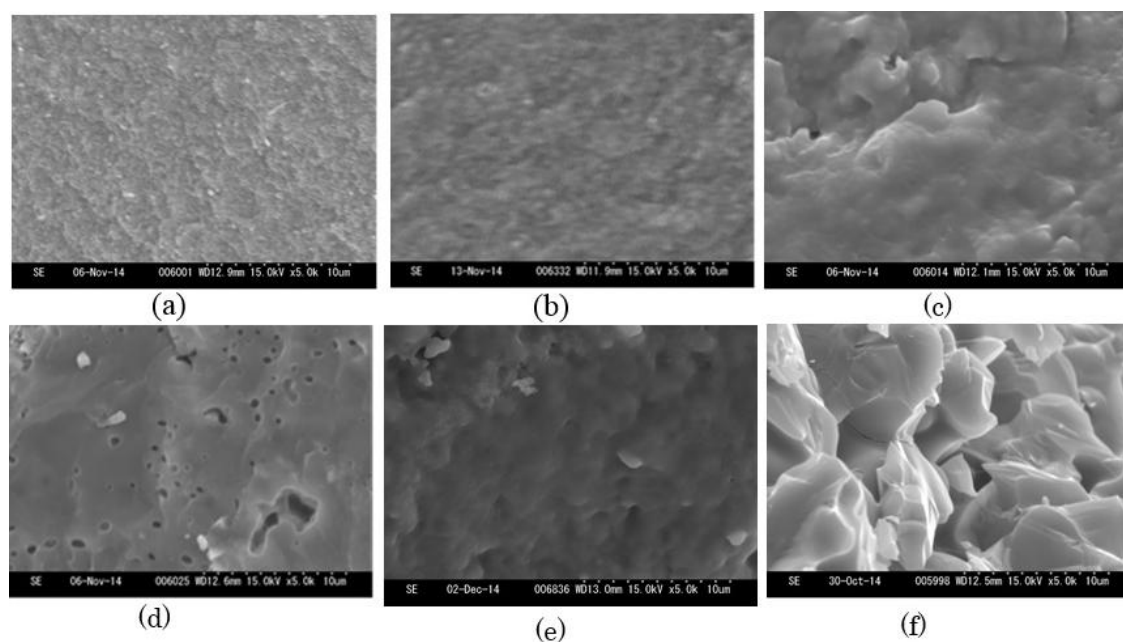


Figure 4 SEM images of silica xerogel loaded by 5 mol% SnO₂ and sintered at temperatures: (a) 800°C; (b) 900°C; (c) 1000°C; (d) 1200°C; (e) 1300 °C; and (f) 1500°C

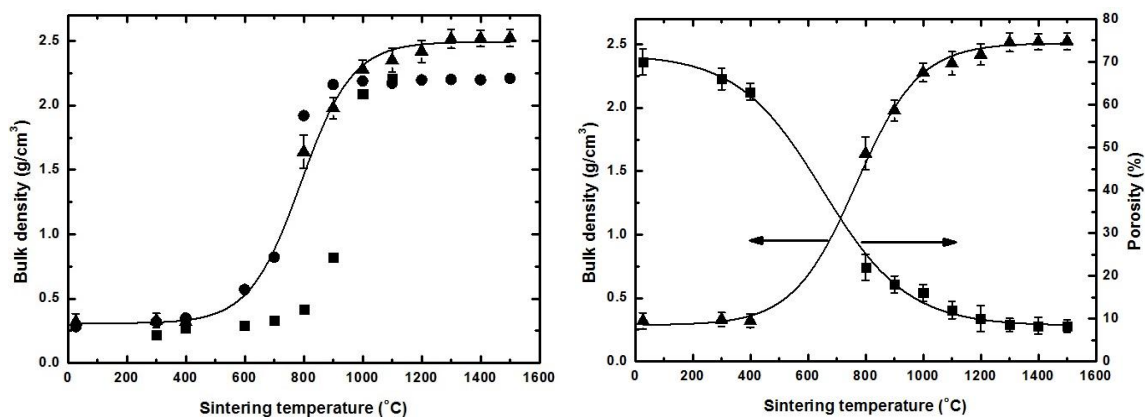


Figure 5 (a) Bulk density of silica sintered by conventional heating (closed square), a volumetric gyrotron heating (closed circle), and composite of silica xerogel and SnO₂ sintered using conventional heating (closed triangle); (b) bulk density and porosity of glass ceramic developed from silica xerogel and SnO₂

Figure 5a shows the bulk density and composite of SX and SnO₂ sintered at various temperatures. The density behavior of the composite followed the trend observed for SX. At first, the bulk density increased slowly up to 400°C, followed by a rapid increase up to 800°C. Above 800°C, the densification rate was very slow, and the body showed approximately 20% porosity (Figure 5b). The reason why an increase in sintering temperature causes an aggregation of the bulk density can be explained by considering a viscous liquid phase mechanism in the sintered sample (Kłosek-Wawrzyna, 2013). First, at temperatures lower than 400°C, a small increase in the bulk density is attributed to the reduction of porosity. These pores are ascribed to the empty sites left by evaporated water and to some residues of PVA, as well as to the combusted residual organics when the sintering process takes place (James, 1988). During the sintering process, at this temperature, silica does not melt into the pockets of a viscous liquid phase within the pores of the ceramic bodies. In the temperature range from 1000°C to 1500°C, the bulk density of silica xerogel/SnO₂ composite increases from 2.3 g/cm³ to 2.5 g/cm³, which is higher than the density of SX alone (about 2.2 g/cm³). Combining these observations with the XRD, FTIR, and SEM results, the increase in density can be explained by an increased degree of crystallinity of SnO₂ in the silica xerogel composite. This crystallization significantly affects the grain growth, while the sintering process provides the necessary energy to bond the particles together and eventually remove the porosity.

4. CONCLUSION

A SnO₂-glass composite was successfully produced from SnO₂ and silica xerogel powder converted from sago waste ash, by controlling the sintering temperature. The results presented in this work show that an incorporation of 5 mol% SnO₂ into silica xerogel has an appreciable effect on the bulk density at temperatures from 1000°C to 1500°C. It was found that the density correlates well with the sintering temperature. When the density of the sample approaches values of about 2.5 g/cm³, the densification rate begins to level off, resulting in a plateau at about 1300°C to 1500°C. In this temperature range, the observed enlargement of the density is accompanied by an increase in crystallization and a decrease in porosity. Compared with the silica xerogel glass composite sintered without SnO₂, the new material has a density which is higher by 14%.

5. ACKNOWLEDGEMENT

This work was partially supported by the Directorate of Research Development and Community Service, Directorate of Higher Education, at the Ministry of Research, Technology and Higher Education, Republic of Indonesia under the Project of International Research Collaboration and Scientific Publication, Number: 1140/D3/PL/2015, and the Research Center of Far Infrared Region (FIR Center), University of Fukui, Japan.

6. REFERENCES

- Affandi, S., Setyawan, H., Winardi, S., Purwanto, A., Balgis, R., 2009. A Facile Method for Production of High-purity Silica Xerogels from Bagasse Ash. *Advanced Powder Technology*, Volume 20, pp. 468–472
- Aripin, H., Mitsudo, S., Prima, E.S., Sudiana, I.N., Tani, S., Sako, K., Fujii, Y., Saito, T., Idehara, T., Sano, S., Sunendar, B., Sabchevski, S., 2012. Structural and Microwave Properties of Silica Xerogel Glass-ceramic Sintered by Sub-millimeter Wave Heating using a Gyrotron. *Journal of Infrared, Millimeter and Terahertz Waves*, Volume 33, pp. 1149–1162
- Aripin, H., Mitsudo, S., Sudiana, I.N., Tani, S., Sako, K., Fujii, Y., Saito, T., Idehara, T., Sabchevski, S., 2011. Rapid Sintering of Silica Xerogel Ceramic Derived from Sago Waste

- Ash using Submillimeter Wave Heating of a 300 GHz CW Gyrotron. *Journal of Infrared, Millimeter and Terahertz Waves*, Volume 32, pp. 867–876
- Aripin, H., Mitsudo, S., Sudiana, I.N., Prima, E.S., Sako, K., Fujii, Y., Saito, T., Idehara, T., Sano, S., Sunendar, B., Hernawan, H., Sabchevski, S., 2013. Microstructural and Thermal Properties of Nanocrystalline Silica Xerogel Powders Converted from Sago Waste Ash Material. *Material Science Forum*, Volume 737, pp. 110–118
- Díaz-Flores, L.L., Garnica-Romo, M.G., González-Hernández, J., Yáñez-Limón, J.M., Vorobiev, P., Vorobiev, Y.V., 2007. Formation of Ag-Cu Nanoparticles in SiO₂ Films by Sol-gel Process and their Effect on the Film Properties. *Physica Status Solidi*, Volume 4, pp. 2016–2020
- Gaber, A., Abdel-Rahim, M.A., Abdel-Latif, A.Y., Abdel-Salam, M.N., 2014. Influence of Calcination Temperature on the Structure and Porosity of Nanocrystalline SnO₂ Synthesized by a Conventional Precipitation Method. *International Journal of Electrochemical Science*, Volume 9, pp. 81–95
- James, P.F., 1988. The Gel to Glass Transition: Chemical and Microstructural Evolution. *Journal of Non-Crystalline Solids*, Volume 100, pp. 93–114
- Jung, H.Y., Gupta, R.K., Oh, E.O., Kim, Y.H., Whang, C.M., 2005. Vibrational Spectroscopic Studies of Sol-gel Derived Physical and Chemical Bonded ORMOSILs. *Journal of Non-Crystalline Solids*, Volume 351, pp. 372–379
- Kim, B.H., Moon, S., Paek, U.C., Han, W.T., 2006. All Fiber Polarimetric Modulation using an Electro-optic Fiber with Internal Pb-Sn Electrodes. *Optics Express*, Volume 14, pp. 11234–11241
- Kłosek-Wawrzyna, E., Małolepszya, J., Murzyn, P., 2013. Sintering Behavior of Kaolin with Calcite. *Procedia Engineering*, Volume 57, pp. 572–582
- Kose, H., Aydin, A.O., Akbulut, H., 2014. The Effect of Temperature on Grain Size of SnO₂ Nanoparticles Synthesized by Sol-gel Method. *Acta Physica Polonica A*, Volume 125, pp. 345–347
- McCarthy, G., Welton, J., 1989. X-ray Diffraction Data for SiO₂, Powder Diffraction. Volume 4, pp. 156–159
- Tan, L., Wang, L., Wang, Y., 2011. Hydrothermal Synthesis of SnO₂ Nanostructures with Different Morphologies and their Optical Properties. *Journal of Nanomaterials*, Volume 2011, pp. 1–10
- Wagh, P.B., Ingale, S.V., 2002. Comparison of some Physico-chemical Properties of Hydrophilic and Hydrophobic Silica Aerogels. *Ceramic International*, Volume 28, pp. 43–50
- Yang, S., Gao, L., 2006. Facile and Surfactant-free Route to Nanocrystalline Mesoporous Tin Oxide. *Journal of the American Ceramic Society*, Volume 89, pp. 1742–1744